

# Non-propagating Fatigue Cracks in an Aluminium- $\frac{1}{2}\%$ Magnesium Alloy

M. A. WILKINS,\* G. C. SMITH

*Department of Metallurgy, University of Cambridge, UK*

Non-propagating fatigue cracks have been observed at the roots of sharp notches in specimens of a single-phase Al- $\frac{1}{2}\%$  Mg alloy. The rate of fatigue crack growth, and the extent of cyclic deformation on either side of the crack, decrease with increase in length of crack. The process of formation of non-propagating cracks can be repeated in the same specimen by means of intermediate anneals. The results are discussed in terms of the cyclic strain-hardening of the material.

## 1. Introduction

The occurrence of non-propagating fatigue cracks at stress-raisers in a variety of materials, under service conditions and in laboratory tests, has been recognised for many years. These cracks are generally short, occur only at sharp notches, and can lie dormant for millions of cycles after growing to their final length in many fewer stress reversals.

Frost [1, 2] showed that such cracks can occur at notch roots in mild steel and an aluminium alloy, and that they propagate if the stress is raised above a critical value, which is independent of notch root radius. He suggested that the cracks became non-propagating once they had grown out of the region of stress concentration associated with the starter-notch, and pointed out that the plastic zone size at the crack tip would be very small compared with that due to the notch.

Coffin [3] utilised a result of Frost [4] which indicated that a finite notch root radius results in minimum fatigue strength, and suggested that this was due to a more rounded notch being able to accommodate completely reversed cyclic deformation, while a very sharp notch cannot, due to the notch faces coming together in compression. In the case of non-propagating cracks it was argued that with moderately sharp notches, the full cyclic strain range could be accommodated at the notch root, but that this would not be true once the crack had formed, so that the crack would slow down.

Hardrath and McEvily [5] calculated an

“effective radius” of a crack tip, based on a modification of Neuber’s [6] elemental block method of analysis of the stress field at a crack tip, and showed that fatigue crack propagation rate data could be successfully correlated if the effective radius was considered to be a constant for the material. If a crack initiated at a notch of root radius smaller than the effective radius of the crack tip, then the crack would subsequently become non-propagating.

Metallurgical suggestions for the formation of non-propagating cracks include (a) that the crack tip deformation becomes contained entirely within a single subgrain surrounding the crack tip [7, 8], (b) that cracks are arrested at grain-boundaries, provided that the grain size is sufficiently small [9, 10], (c) that the formation of a compact surface oxide film at a crack tip in aluminium effectively stops the motion of dislocations through the surface [11], and (d) that cracks formed at ferrite/pearlite interfaces in medium carbon steel may not be able to spread through the ferrite matrix [12].

In the present work, non-propagating cracks have been observed in a high-purity Al- $\frac{1}{2}\%$  Mg alloy, and have been examined using a variety of experimental techniques. Many of the hypotheses mentioned above have been shown to be inapplicable, and the results are discussed in terms of the cyclic strain-hardening behaviour of the material.

## 2. Experimental Procedure

Sharply-notched polycrystalline specimens, fig.

\* Now at National Physical Laboratory, Teddington, Middlesex.

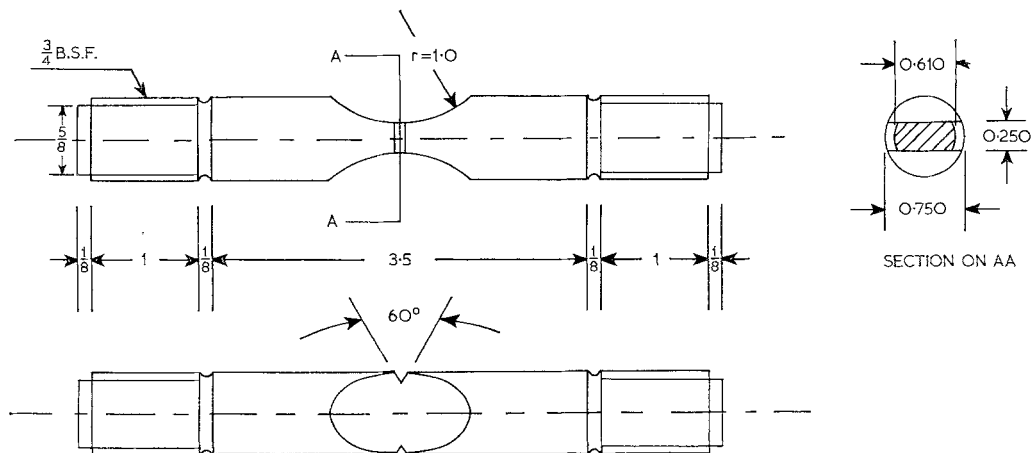


Figure 1 Fatigue test specimen. All dimensions in inches; 1 in. = 2.54 cm.

1, were machined from  $\frac{3}{4}$  in. diameter bar of a high-purity Al- $\frac{1}{2}\%$  Mg alloy (table I). The notch root radius was 0.0005 in. After machining, specimens were annealed for 1 h at 450° C *in vacuo* to obtain a linear intercept grain size of 0.015 in.

TABLE I Spectrographic analysis: of the high purity aluminium/magnesium alloy

Element	Weight percentage	
Mg	0.50	
Cu	0.004	
Fe	Sl. Tr.	~ 0.002
Si	Sl. Tr.	~ 0.002
Mn	Sl. Tr.	~ 0.002
Ni	N.D.	< 0.01 if any
Pb	N.D.	< 0.01 if any
Cr	N.D.	< 0.01 if any
Zn	N.D.	< 0.005 if any
Ti	N.D.	< 0.002 if any
Al	Remainder	

Specimens were cycled in constant load push-pull direct stress with zero mean load, in a Losenhausen UHW6 fatigue machine operating at 1500 cpm.

For surface metallographic and crack growth rate observations, the sides of the specimens between the edge notches were electropolished, shown as area A in fig. 2. Surface crack-propagation rates were determined by means of a binocular microscope and calibrated eyepiece. Cracks propagated from both edge-notches so that a total of four measurements of crack length were made on each sample.

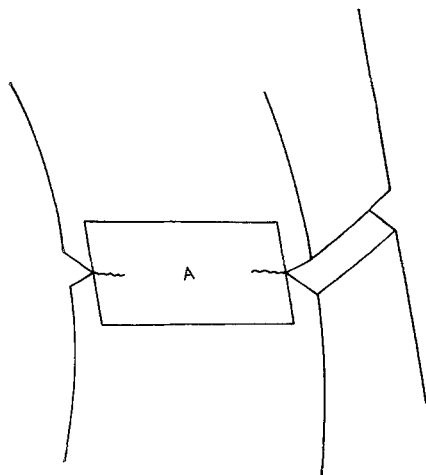


Figure 2 Diagram showing the relative positions of the fatigue crack, the notch, and the electropolished side free surface of the specimen, area A.

Dislocation structures around the fatigue crack were examined by means of thin foil transmission electron microscopy, using a technique which has been reported elsewhere [13].

### 3. Results

#### 3.1. Crack Growth Rate Curves

Specimens were tested at three alternating stresses, each test being run to a life of  $10^7$  cycles. Typical plots of crack length versus cycles for individual cracks are shown in fig. 3. Growth rate was high in the first  $10^6$  cycles, but subsequently decreased to very low levels. One test was run to a total of  $2.5 \times 10^7$  cycles, but no further change in crack length could be detected.

Several tests were carried out at each stress level, and the average length of crack at  $10^7$  cycles plotted as a function of stress, fig. 4.

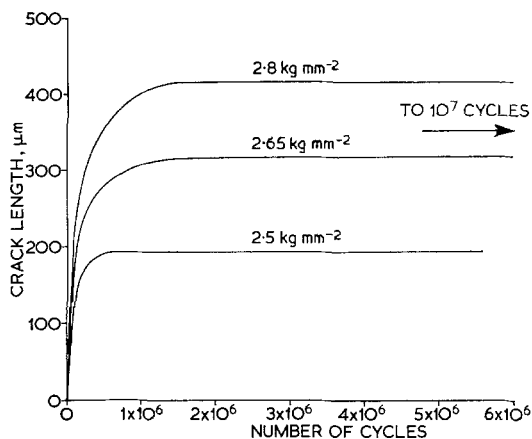


Figure 3 The relationship between crack length and number of cycles elapsed for typical specimens tested at different alternating stresses.

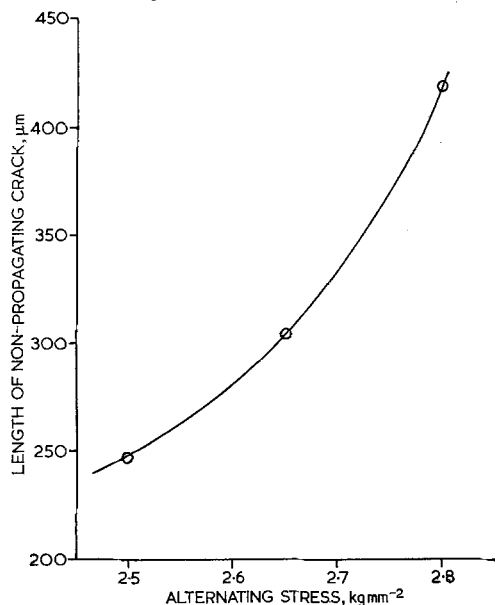


Figure 4 The average length of non-propagating cracks as a function of alternating stress.

To demonstrate that the crack length measured on the surface was representative of the crack length across the thickness of the specimen, one specimen was cycled at  $0 \pm 2.8 \text{ kg mm}^{-2}$  to produce a non-propagating crack, and then broken at a high cyclic stress. A constant length of crack across the whole fractured cross-section is shown in fig. 5, the line of demarcation between the partially intercrystalline low stress area and

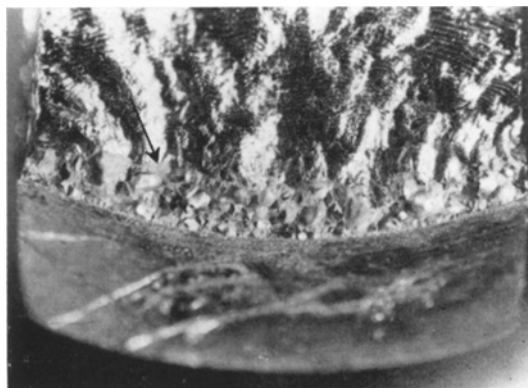


Figure 5 The fracture surface, beyond the notch root, of a specimen broken at high stress after the formation of a non-propagating crack. The line of demarcation between the low and high stress regions is indicated by the arrow ( $\times 8$ ).

the stage II striations exhibited in the high stress region being indicated by the arrow.

### 3.2. Annealing Behaviour

Several specimens were tested at two different stress levels, intermediate annealing treatments being carried out at  $450^\circ \text{C}$  *in vacuo* for 1 h, at intervals of  $10^7$  cycles.

Two specimens were cycled at  $0 \pm 2.8 \text{ kg mm}^{-2}$  for  $10^7$  cycles, annealed, and re-tested with the same load. In each case, further crack-propagation took place to fracture.

This procedure was repeated for two specimens cycled at  $0 \pm 2.5 \text{ kg mm}^{-2}$ . After annealing, further crack growth took place, but eventually the cracks became non-propagating. The treatment was repeated a second time, with the same result, fig. 6.

To check that the further crack-propagation did not take place due to crack tip stress relaxation when the specimens were unloaded and removed from the fatigue machine, one specimen was cycled for  $10^7$  cycles at  $0 \pm 2.5 \text{ kg mm}^{-2}$ , removed from the machine, left at room temperature for 1 h, replaced in the machine, and retested. No further crack propagation took place, over  $10^7$  cycles.

### 3.3. Surface Deformation Structure

The deformation structure associated with the cracks was examined optically on the electro-polished side surfaces of the specimens. All cracks were surrounded by an array of slip bands characteristic of low strain fatigue [14]. In

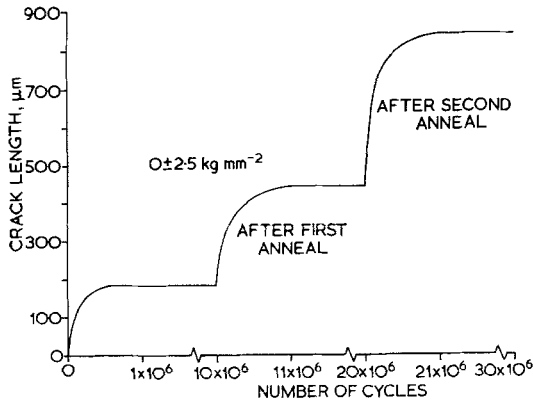


Figure 6 The relationship between crack length and number of cycles elapsed, for a specimen cycled at  $0 \pm 2.5 \text{ kg mm}^{-2}$  with intermediate anneals at intervals of  $10^7$  cycles.

many cases, the distance to which the slip band structure extended to the sides of the crack, in the direction of the stress axis, decreased with increasing distance from the notch root, fig. 7.

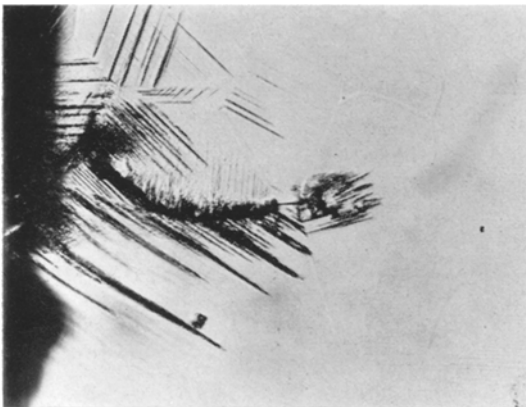


Figure 7 The deformation structure associated with a non-propagating crack observed on the side free surface of the specimen. Stress axis vertical ( $\times 40$ ).

Only very rarely was any significant amount of deformation, in the form of surface slip bands, observed ahead of the main crack, once the crack had become non-propagating.

The surface slip band distribution around the cracks developed in the annealing experiments described in section 3.2 above was also examined. It was observed that the distribution of slip behind the position originally taken up by the tip of the non-propagating crack was not altered

when cycling was restarted after the annealing treatment; this behaviour confirmed the position of the crack tip as being close to the farthest limit of slip band deformation. The general distribution of slip in each successive period of crack growth is similar to that observed after the first period of cycling. These points are illustrated in fig. 8 which shows the development of the crack to which the curves of fig. 6 relate.

### 3.4. Dislocation Structures

The dislocation arrangements around non-propagating cracks produced at  $0 \pm 2.8 \text{ kg mm}^{-2}$  were examined, cracks produced at lower stresses being too short for the experimental technique to be readily applied.

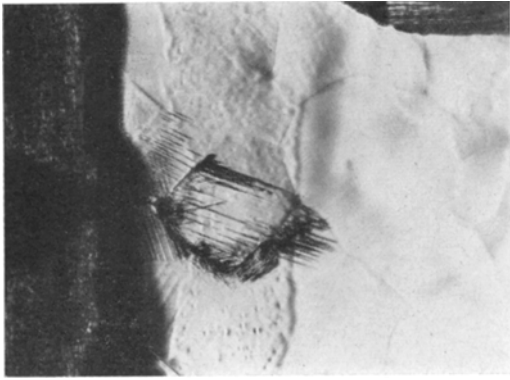
To the side of the crack, behind the crack tip, dislocation structures were observed which were similar to those observed ahead and to the side of a propagating fatigue crack in the same material [15]. Thus, remote from the crack, patches of elongated dislocation loops were observed (fig. 9); closer to the crack, rearrangement of the loops into cell walls took place (fig. 10) while at the side of the crack itself, a cell structure due to spontaneous recovery processes was present (fig. 11).

The extent of each type of dislocation structure outwards from the sides of the cracks in the direction of the stress axis reflected the observations of slip band distribution on the side free surfaces of the specimens, i.e. the distance to the side of the crack at which any given structure was observed decreased with increasing distance from the notch root, as illustrated schematically in fig. 12. Thus at  $100 \mu\text{m}$  back from the tip of the crack, the cell structure extended approximately  $30 \mu\text{m}$  from the crack side, and the recovered cell structure  $8 \mu\text{m}$ . At a distance of  $30 \mu\text{m}$  from the crack tip, the corresponding figures were approximately  $10 \mu\text{m}$  and  $1 \mu\text{m}$ .

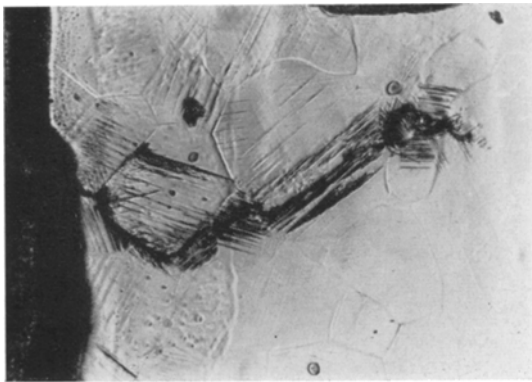
The extent of deformation was also restricted ahead of the crack tip. Fig. 13 shows an elongated loop structure  $18 \mu\text{m}$  ahead of the crack; no cell structures were observed in this region, but owing to difficulties introduced into the experimental technique as a consequence of the shortness of the crack, no micrographs were obtained from regions within a few microns of the tip.

## 4. Discussion

Previous experiments [15] in which the dislocation structures in the vicinity of a propagating fatigue crack in the Al- $\frac{1}{2}$ % Mg alloy have been



(a)



(b)



(c)

*Figure 8* The surface slip band distribution around non-propagating cracks developed in the annealing experiments illustrated in fig. 6. (a) After  $10^7$  cycles ( $\times 62$ ); (b) after the first anneal, and a further  $10^7$  cycles ( $\times 62$ ); (c) after the second anneal, and a further  $10^7$  cycles ( $\times 31$ ). Stress axis vertical.

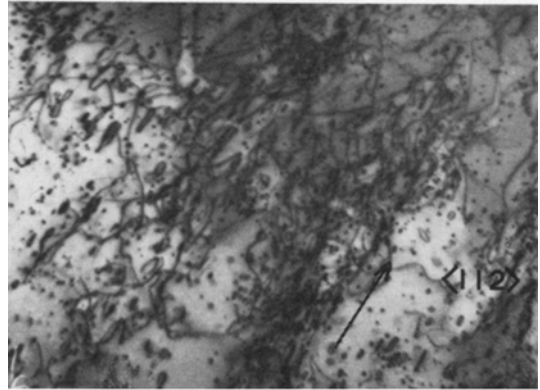


*Figure 9* Dislocation loops, elongated in  $\langle 112 \rangle$ , observed in positions remote from the crack ( $\times 10\,800$ ).

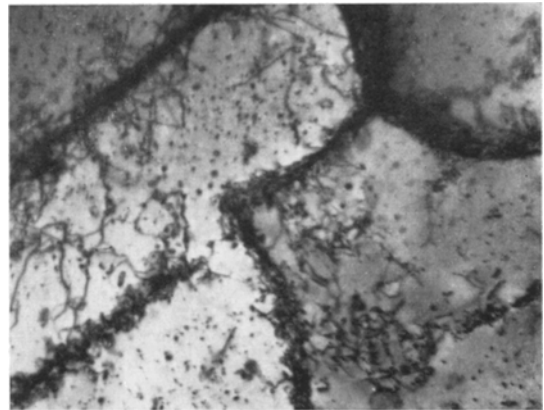


*Figure 10* Cellular dislocation arrangements observed close to the crack ( $\times 10\,800$ ).

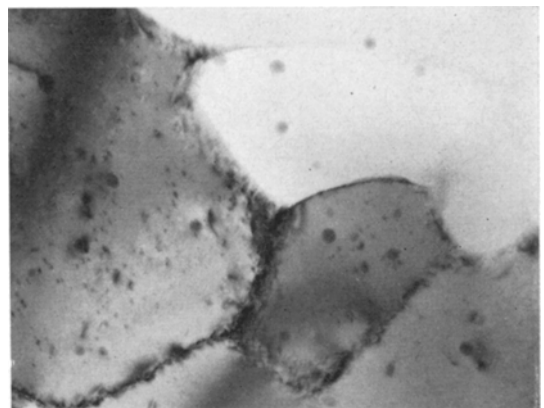


*Figure 11* A cellular structure, due to spontaneous recovery processes, observed at the side of the crack ( $\times 10\,800$ ).

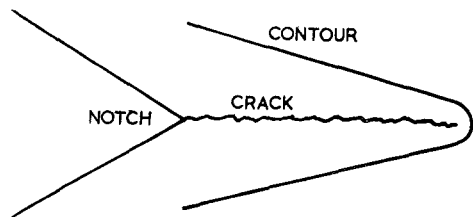


Figure 12 A schematic illustration of the shape of the deformation zone associated with a non-propagating crack. The contour connects positions exhibiting similar dislocation structures.

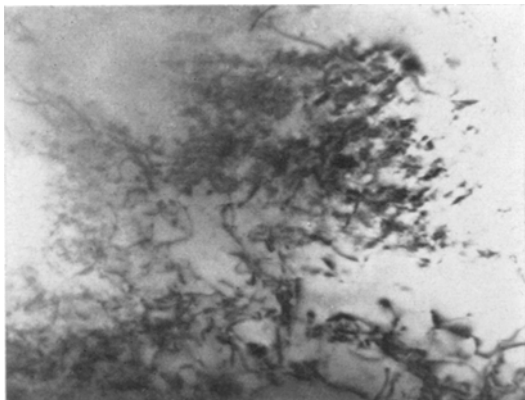


Figure 13 A dislocation loop structure observed 18  $\mu\text{m}$  ahead of a non-propagating crack ( $\times 10\,800$ ).

examined have revealed that the zone of crack tip deformation extends to considerable distances ahead of the crack tip, over a wide range of crack-propagation rates. The present experiments indicate a much more restricted amount of deformation in this region together with a deformation zone to the crack sides tapering in the direction of crack extension. These observations are confirmed by the surface slip band distribution. The decreasing spread of deformation around the crack, with increasing crack length, occurs simultaneously with a decelerating crack growth rate.

Cracks were not observed to terminate at metallurgical features, such as grain-boundaries, nor was crack-branching observed at the tips of non-propagating cracks – a mechanism for crack arrest which has been suggested [16]. Indeed, the crack tip was always sharp, with a tip radius of the order of a tenth of a micron.

The annealing experiments demonstrate that non-propagating cracks can develop from pre-existing fatigue cracks as well as from machined notches. This suggests, in this instance, that the

ability of the relatively rounded notch root to permit fully reversed plastic deformation does not contribute significantly to the initial crack-propagation rate [3]. The suggestion [17] that the annealing process may relax stresses around the crack and hence cause blunting of the crack tip, effectively creating a new notch, is not considered likely; during a control experiment, the crack did not show any fine-scale widening when examined by thin-foil transmission electron microscopy, the position of the crack tip during the annealing treatment being reasonably well defined by a marked decrease in dislocation density behind this point. The fact that further crack-propagation becomes possible after annealing does suggest, however, that cyclic strain hardening is responsible for the reduction of the crack-propagation rate to very low levels.

There is little accumulation of deformation structure directly ahead of the crack tip, so the effect of this in making crack-propagation inherently more difficult than in material of lower dislocation density is likely to be small. It is suggested, therefore, that cyclic strain-hardening is the main factor in causing crack arrest by the effect it has on the properties of the matrix material remote from the crack. For small scale yielding ahead of a crack in a material stressed well below its general yield stress, the extent of plastic deformation around the crack tip, and hence the strain at the crack tip, will depend on the yield stress [18]. In the present case, where some yielding has taken place across the whole section, the extent of crack tip deformation will be a complex function of the yield stress and the rate of cyclic strain-hardening. In general, however, crack tip deformation will decrease with increase in both of these parameters.

The cyclic strain-hardening response of the present Al- $\frac{1}{2}\%$  Mg alloy does not show a clearly defined saturation stress for tests carried out at constant cyclic strain amplitude [19], fig. 14. These results are similar to ones for pure aluminium [20, 21]. During load cycling, continual strain-hardening will therefore occur throughout the specimen cross-section resulting in a steady reduction of plastic strain, generally, and at the crack tip.

Al-Mg alloys also undergo dynamic strain ageing [22], and if this occurred in fatigue, further hardening would result. The curves of fig. 14, which do not show saturation of strain-hardening, may in fact be a consequence of strain-ageing.

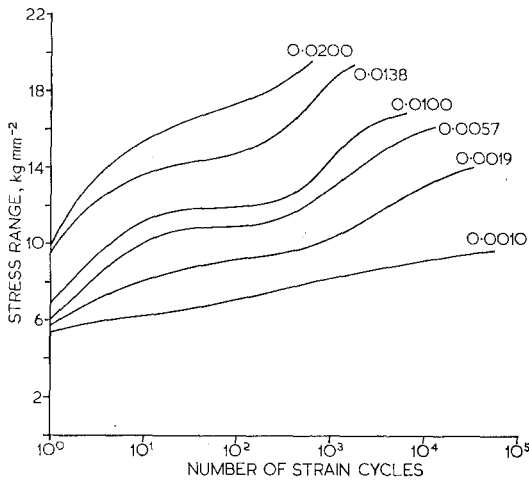


Figure 14 The cyclic strain-hardening response of the Al- $\frac{1}{2}$ % Mg alloy, measured as the stress range required to enforce the strain limits. Semi-range of total strain shown adjacent to each curve.

The continued hardening of the matrix remote from the crack tip will steadily reduce the crack opening displacement and the crack-propagation rate. The observation that the tip of the crack is sharp suggests, however, that a small amount of plastic strain must be accommodated there in each cycle. If however this is small it may take place by reversible dislocation motion so that no contribution is made to crack extension. Any irreversible components of slip would be expected to provide crack growth, but if these are small, crack growth would only be observed over very long lives, which are not normally investigated.

### Acknowledgement

The authors are indebted to Messrs S. D. Charter and S. W. Childerley for considerable help with the experimental work, and to the British Non-Ferrous Metals Research Association for the

spectrographic analysis. One of the authors (M.A.W.) wishes to thank the Ministry of Technology for financial support.

### References

1. N. E. FROST, *Proc. IME* **173** (1959) 35.
2. *Idem*, *J. Mech. Eng. Sci.* **2** (1960) 109.
3. L. F. COFFIN, *Proc. Am. Soc. Test. Mat.* **58** (1958) 570.
4. N. E. FROST, *Aeronautical Quarterly* **8** (1957) 1.
5. H. F. HARDRATH and A. J. MCEVILY, Symposium on Crack Propagation, Cranfield, 1961, p. 231.
6. H. NEUBER, "Theory of Notch Stresses" (Springer, Berlin, 1937).
7. J. HOLDEN, *Phil. Mag.* **6** (1961) 547.
8. D. H. AVERY and W. A. BACKOFEN, International Conference on Fracture of Solids (Gordon and Breach, New York, 1963).
9. P. G. FORREST and A. E. L. TATE, *J. Inst. Met.* **93** (1965) 438.
10. G. OATES and D. V. WILSON, *Acta Met.* **12** (1964) 21.
11. R. W. LARDNER, *Phil. Mag.* **17** (1968) 71.
12. N. J. WADSWORTH, *ibid* **6** (1961) 397.
13. P. N. T. UNWIN and M. A. WILKINS, *J. Sci. Inst.* **2** (2) (1969) 736.
14. N. THOMPSON, N. J. WADSWORTH, and N. LOUAT, *Phil. Mag.* **1** (1956) 113.
15. M. A. WILKINS and G. C. SMITH, accepted for publication in *Acta Met.*
16. N. E. FROST and C. E. PHILLIPS, *Proc. Roy. Soc. A242* (1957) 216.
17. A. J. MCEVILY, private communication.
18. J. R. RICE, Fatigue Crack Propagation Symposium, ASTM STP 415, 1967, p. 247.
19. M. A. WILKINS, Ph.D. Thesis, University of Cambridge, 1969.
20. L. F. COFFIN and J. F. TAVERNELLI, *Trans. AIME* **215** (1959) 794.
21. R. J. HARTMANN, *J. Appl. Phys.* **36** (1965) 1751.
22. A. T. THOMAS, *Acta Met.* **14** (1966) 1363.

Received 8 December 1969 and accepted 20 February 1970.